

Ductility of bulk nanocrystalline composites and metallic glasses at room temperature

Cang Fan^{a)} and Akihisa Inoue^{b)}

Japan Science and Technology Corporation, Sendai 982-0807, Japan

(Received 17 February 2000; accepted for publication 3 May 2000)

Mechanical properties of bulk $\text{Zr}_{60}\text{Cu}_{20}\text{Pd}_{10}\text{Al}_{10}$ nanocrystalline composite and $\text{Zr}_{55}\text{Ni}_5\text{Cu}_{30}\text{Al}_{10}$ metallic glass were measured by compression tests at room temperature. The $\text{Zr}_{60}\text{Cu}_{20}\text{Pd}_{10}\text{Al}_{10}$ as-quenched alloy obviously exhibits plastic strain while no distinct plastic deformation is recognized in the $\text{Zr}_{55}\text{Ni}_5\text{Cu}_{30}\text{Al}_{10}$ metallic glass. Moreover, the plastic strain increased by increasing the volume fraction of nanocrystals and achieved maximum value in the early stage of the nanocrystallization. High-resolution electron microscopy showed that, different from the microstructure of $\text{Zr}_{55}\text{Ni}_5\text{Cu}_{30}\text{Al}_{10}$ metallic glass, nanocrystals with main grain sizes of about 2 nm were embedded in the amorphous matrix of the bulk $\text{Zr}_{60}\text{Cu}_{20}\text{Pd}_{10}\text{Al}_{10}$ alloy which showed the maximum plastic strain. © 2000 American Institute of Physics. [S0003-6951(00)01027-5]

A high degree of crystallization leads to embrittlement, but if it can be arrested when the crystallites are of only nanometer dimensions, the resulting nanocrystalline composites (materials with nanoparticles dispersed in an amorphous matrix) actually have greater tensile strength than the original amorphous materials.^{1–6} However, with bulk nanocrystalline composites a decrease in ductility but with a concurrent increase in strength with increasing volume fraction of nanocrystals is observed.⁵ This behavior was interpreted to be due to the supposed brittleness of the precipitated nanocrystals.

There is, consequently, much interest in realizing the variation in ductility of nanocrystalline composites and amorphous materials. In the present work we investigated the mechanical properties measured by compression tests and the microstructures observed by high-resolution electron microscopy in bulk $\text{Zr}_{60}\text{Cu}_{20}\text{Pd}_{10}\text{Al}_{10}$ nanocrystalline composite and $\text{Zr}_{55}\text{Ni}_5\text{Cu}_{30}\text{Al}_{10}$ metallic glasses. In contrast to investigations reported previously, we found that nanoparticles leading to an increase of both ductility and strength.

$\text{Zr}_{60}\text{Cu}_{20}\text{Pd}_{10}\text{Al}_{10}$ and $\text{Zr}_{55}\text{Ni}_5\text{Cu}_{30}\text{Al}_{10}$ ingots were initially prepared by arc melting the mixtures of pure metals in a purified argon atmosphere and cast into a copper mold in vacuum. The $\text{Zr}_{60}\text{Cu}_{20}\text{Pd}_{10}\text{Al}_{10}$ alloy crystallizes via precipitation of a metastable phase in the primary crystallization step leading to nanoparticles embedded in an amorphous matrix.^{3,4} The $\text{Zr}_{55}\text{Ni}_5\text{Cu}_{30}\text{Al}_{10}$ alloy shows a typical large glass-forming ability.⁷ X-ray measurements were performed on as-cast specimens to check the amorphiticity of the sample. The amorphous alloys were partially crystallized by isothermal annealing in the supercooled liquid region and the volume fraction (V_f) of nanocrystals was estimated by differential scanning calorimetry (i.e., V_f proportional to the ribbon's heat release upon partial crystallization). Microstructures of the specimens were examined by high-

resolution electron microscopy (JEM-3000F, operated at 300 kV). The mechanical properties were measured by compression tests using cylinders 2.0 mm in diameter and 4.2 mm long at a strain rate of $4.4 \times 10^{-4} \text{ s}^{-1}$ at room temperature. Young's modulus was measured by a strain gage. The shear bands of samples were investigated by scanning electron microscopy.

Figure 1 shows the compressive stress–strain curves: (a) for bulk $\text{Zr}_{55}\text{Ni}_5\text{Cu}_{30}\text{Al}_{10}$ amorphous alloy; (b), (c), (d), and (e) for as-quenched and annealed bulk $\text{Zr}_{60}\text{Cu}_{20}\text{Pd}_{10}\text{Al}_{10}$ alloys. The stress–strain relation is linear up to about 1.8%–2% compressive strain. Beyond this strain plastic deformation sets in as evidenced by unloading the specimen. No distinct plastic deformation is observed in the $\text{Zr}_{55}\text{Ni}_5\text{Cu}_{30}\text{Al}_{10}$ amorphous alloy, but the $\text{Zr}_{60}\text{Cu}_{20}\text{Pd}_{10}\text{Al}_{10}$ as-quenched alloy exhibits a plastic strain to failure (after yielding) being several times that of the $\text{Zr}_{55}\text{Ni}_5\text{Cu}_{30}\text{Al}_{10}$ amorphous reference [Figs. 1(a) and 1(b)], indicating the improved ductility of the nanocrystal-forming alloy. Moreover, in the partially crystallized $\text{Zr}_{60}\text{Cu}_{20}\text{Pd}_{10}\text{Al}_{10}$ alloy at $V_f = 27\%$ [Fig. 1(c)], the curve shows a further improved plas-

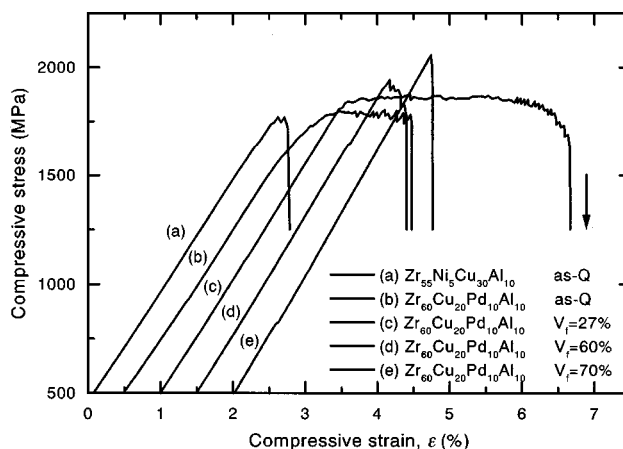


FIG. 1. Compressive stress–strain curves at room temperature: (a) for bulk $\text{Zr}_{55}\text{Ni}_5\text{Cu}_{30}\text{Al}_{10}$ metallic glass; (b), (c), (d), and (e) for as-quenched and nanocrystalline bulk $\text{Zr}_{60}\text{Cu}_{20}\text{Pd}_{10}\text{Al}_{10}$.

^{a)}Electronic mail: cangfan@sendai.jst.go.jp

^{b)}Also at: Institute for Materials Research, Tohoku University, Sendai 980-8577, Japan.

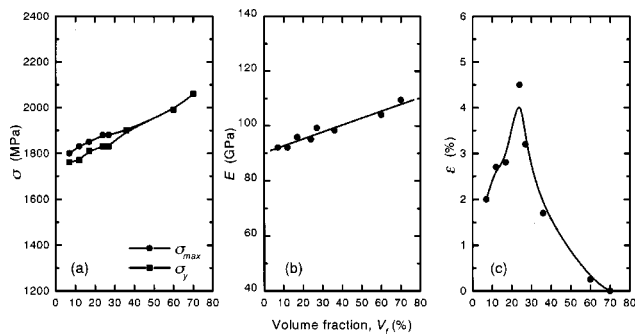


FIG. 2. Mechanical properties: (a) compressive yield strength σ_y and the maximum strength σ_{max} ; (b) Young's modulus E , and (c) plastic strain ϵ_p to failure (after yielding) of $Zr_{60}Cu_{20}Pd_{10}Al_{10}$ alloy with different volume fraction of nanocrystals.

tic strain being close to two times larger than that of the corresponding as-quenched alloy [Fig. 1(b)]. In the $V_f = 60\%$ sample [Fig. 1(d)] plastic strain is smaller than that of the as-quenched one [Fig. 1(b)] but still larger than that of the $Zr_{55}Ni_5Cu_{30}Al_{10}$ amorphous reference [Fig. 1(a)]. Further increasing V_f to 70%, there is no plastic strain before fracture, but it shows the largest fracture stress [Fig. 1(e)].

Mechanical properties of the $Zr_{60}Cu_{20}Pd_{10}Al_{10}$ alloy with different volume fraction of nanocrystals are shown in Fig. 2. It should be mentioned that the magnitude of the enthalpy of the first exothermic peak measured by the differential scanning calorimetry, corresponding with the nanocrystallization^{4,8} for the as-quenched bulk $Zr_{60}Cu_{20}Pd_{10}Al_{10}$ is approximately 7% less than the ribbon one. Thus, it is recognized that nanoparticles of around $V_f = 7\%$ exist in the as-quenched bulk (the existence of the nanoparticles has been confirmed by high-resolution electron microscopy). As shown in Fig. 2(c), the plastic strain ϵ_p to failure is 2.0% for the as-quenched one ($V_f = 7\%$), increases by increasing V_f , and reaches a maximum value of 4.5% at $V_f = 24\%$. Further increasing V_f , the plastic strain starts to decrease again and is about 0% at $V_f = 70\%$. While the measured strains are at variance with previous results,⁵ the generally observed increase in compressive yield strength σ_y , the maximum strength σ_{max} , and Young's modulus E was found in this nanocrystalline alloy as well [Figs. 2(a) and 2(b)]. It also shows that the yield strengths are significantly smaller than the maximum strengths while V_f is below around 35%.

In order to examine the reason for the increased ductility, we have also studied the microstructure of the specimen, which showed the maximum value of plastic strain by high-resolution electron microscopy. Figure 3 shows the images of the annealed specimen with V_f of 24% of the bulk $Zr_{60}Cu_{20}Pd_{10}Al_{10}$ alloy. It shows many fine crystals (circled in Fig 3), which is a metastable compound phase,⁴ dispersed in the amorphous matrix. The size of the particles range mainly from 1 to 2 nm. These particles are spherical, almost no defects are observed within the particles, and the crystal orientation of each particle appears to be completely randomly distributed as well. The microstructure is different from the microstructure of the $Zr_{55}Ni_5Cu_{30}Al_{10}$ alloys, which are purely amorphous.

Macroscopic information about the nature of the plastic deformation of the metallic glass and the nanocrystalline

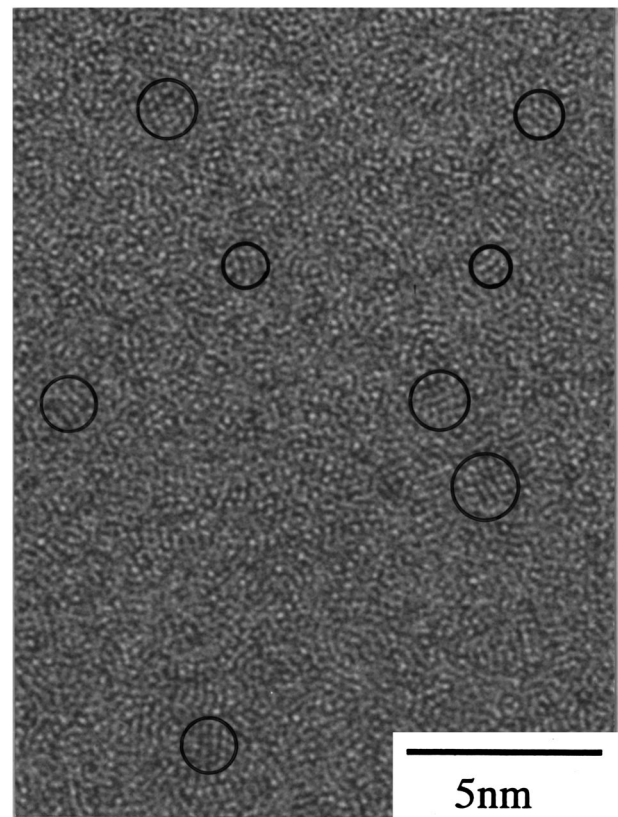


FIG. 3. High-resolution electron microscopy images of the annealed specimen with $V_f = 24\%$ of the bulk $Zr_{60}Cu_{20}Pd_{10}Al_{10}$ alloy. Nanocrystals are circled.

composite were obtained by scanning electron microscopy. Figure 4 shows (a) the surface appearance of a specimen of $Zr_{55}Ni_5Cu_{30}Al_{10}$, and (b) that of an annealed specimen of $Zr_{60}Cu_{20}Pd_{10}Al_{10}$ with $V_f = 24\%$ after fracture, respectively. Many localized slip bands marked by arrows [Fig. 4(b)] are observed clearly in the nanocrystalline specimen and the angle of the slip bands to the compressive is approximately $45^\circ - 50^\circ$. This is quite different to the one of $Zr_{55}Ni_5Cu_{30}Al_{10}$ specimens, where only a few slip bands are found [Fig. 4 (a)]. Together with Fig. 1(c), it suggests that when the yield strength is achieved, the plastic deformation begins and a slip band occurs, but the deformations are not limited in this slip band. Other slip bands occur one after another at different places while the stress increases. The result is that the plastic flow takes place more homogeneously in $Zr_{60}Cu_{20}Pd_{10}Al_{10}$ specimens with $V_f = 24\%$.

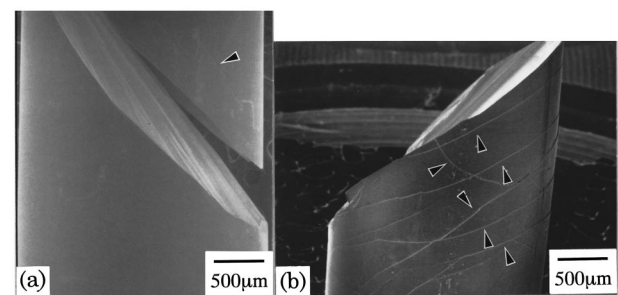


FIG. 4. The nature of the plastic deformation of (a) the $Zr_{55}Ni_5Cu_{30}Al_{10}$ metallic glass and (b) the $Zr_{60}Cu_{20}Pd_{10}Al_{10}$ nanocrystalline composite ($V_f = 24\%$) after fracture observed by scanning electron microscope. Localized shear bands are indicated by arrows.

It is important to understand what causes the above behavior in the $\text{Zr}_{60}\text{Cu}_{20}\text{Pd}_{10}\text{Al}_{10}$ nanocrystalline composite. The above nanocrystal is a metastable compound phase structured by tetragonal $\text{Zr}_2(\text{Cu}, \text{Pd})$ ^{3,4} which is commonly supposed to exhibit large hardness and to be brittle. So far, the increase in strength and concurrent decrease in ductility in partially crystallized bulk nanocrystalline composites was attributed to the supposed hardness and brittleness of the nanocrystals.⁵ Upon loading they would not deform and act as obstacles preventing shear bands to move. Thus, the yield stress is raised while at the same time ductility decreases because the shear bands, in which plastic deformation takes place, cannot move freely through the material. While this argument may qualitatively explain the observed increase in strength, it fails to explain the increased ductility in our experiments.

Kung and Foedke⁹ suggest that as the structural scale reduces to the nanometer range, the limits of the conventional descriptions of yielding need to be established, and new mechanisms may come into play at these small dimensions. In addition, the interfacial effects, which are due to the intrinsically high interface-to-volume ratio of the nanostructured materials, can dominate microstructure and properties leading to unusually large strains and frequent stabilization of metastable structures.¹⁰ Nanoparticles with 2.0 nm in diameter have tremendous interface-to-volume ratio of $3 \text{ mm}^2/\text{mm}^3$. Such high interface-to-volume ratio probably leads to mechanical properties different from those of a material with the same metastable phase but of usual grain size. Supposing that the nanocrystals exhibit ductility, in addition to the remaining amorphous phase between nanocrystals deforming locally, the plastic deformation of the composite,

which is thus larger than that of a material with pure amorphous structure, may occur. Since increased ductility was observed when the alloy contained nanocrystalline and amorphous phases, it can be assumed to be attributable to the ductile nature of the nanocrystalline and the remaining amorphous phase. On the other hand, as the nanocrystals are almost without internal defects, i.e., a nearly perfect crystal, the increase of yield strength as a function of V_f of the nanocrystals can happen.

In conclusion, the ductility of the nanocrystal-forming alloys is much better than that of the pure amorphous alloys. The existence of nanocrystals being only a few nanometers in diameter dispersed in an amorphous matrix was found to lead to an increase of both the strength and the ductility with increasing V_f of nanocrystals in early stages of the nanocrystallization in $\text{Zr}_{60}\text{Cu}_{20}\text{Pd}_{10}\text{Al}_{10}$. We suggest that the intrinsically high interface-to-volume ratio of the nanocrystals may lead to improved mechanical properties of the metastable compound and contribute to the increase of ductility.

¹H. Chen, Y. He, G. J. Shiflet, and S. J. Poon, *Nature (London)* **367**, 541 (1994).

²H. Chen, Y. He, G. J. Shiflet, and S. J. Poon, *Scr. Metall. Mater.* **25**, 1421 (1991).

³C. Fan and A. Inoue, *Mater. Trans., JIM* **38**, 1040 (1997).

⁴C. Fan, A. Takeuchi, and A. Inoue, *Mater. Trans., JIM* **40**, 42 (1999).

⁵L. Q. Xing, J. Eckert, W. Loser, and L. Schultz, *Appl. Phys. Lett.* **74**, 664 (1999).

⁶C. Fan, D. V. Louzguine, C. Li, and A. Inoue, *Appl. Phys. Lett.* **75**, 340 (1999).

⁷A. Inoue and T. Zhang, *Mater. Trans., JIM* **37**, 185 (1996).

⁸C. Fan and A. Inoue, *Appl. Phys. Lett.* **75**, 3644 (1999).

⁹H. Kung and T. Foedke, *MRS Bull.* **24**, 14 (1999).

¹⁰B. M. Clemens, H. Kung, and S. A. Barnett, *MRS Bull.* **24**, 20 (1999).